Science Advances
AAAS

advances.sciencemag.org/cgi/content/full/5/6/eaaw0076/DC1

Supplementary Materials for

Enhanced North American carbon uptake associated with El Niño

Lei Hu*, Arlyn E. Andrews*, Kirk W. Thoning, Colm Sweeney, John B. Miller, Anna M. Michalak, Ed Dlugokencky, Pieter P. Tans, Yoichi P. Shiga, Marikate Mountain, Thomas Nehrkorn, Stephen A. Montzka, Kathryn McKain, Jonathan Kofler, Michael Trudeau, Sylvia E. Michel, Sébastien C. Biraud, Marc L. Fischer, Doug E. J. Worthy, Bruce H. Vaughn, James W. C. White, Vineet Yadav, Sourish Basu, Ivar R. van der Velde

*Corresponding author. Email: lei.hu@noaa.gov (L.H.); arlyn.andrews@noaa.gov (A.E.A.)

Published 5 June 2019, *Sci. Adv.* **5**, eaaw0076 (2019)
DOI: 10.1126/sciadv.aaw0076

This PDF file includes:

Fig. S12. Correlations between monthly NEE anomalies and monthly anomalies of hydrological variables (precipitation, relative humidity, vapor pressure deficit, and soil moisture) and the sensitivity of NEE anomalies to hydrological conditions.
Fig. S13. Correlations between NEE anomalies and anomalies of air temperature in spring and summer, and the sensitivity of NEE anomalies to air temperature.
Fig. S14. Difference of anomalies of air temperature, precipitation, relative humidity, vapor pressure deficit, and soil moisture between El Niño and non El Niño (neutral and La Niña) periods.
Fig. S15. Correlations between the ONI and 3-month average anomalies of area-weighted average precipitation, RH, SM, and VPD over boreal (blue symbols) and temperate (red symbols) North America with ±10-month time lags.
Fig. S16. Correlations between the ONI and 3-month average anomalies of area-weighted average precipitation, RH, SM, and VPD over temperate North America for every 20 years between 1950 and 2016.
Fig. S17. Atmospheric CO_2 observations between 2007 and 2015 with different colors indicating their total sensitivity [sumH, ppm (μmol m^{-2} s^{-1})$^{-1}$] to North American land fluxes.
Fig. S18. Observed CO_2 mole fractions for observations used in this analysis and their associated background estimates.
Table S1. Site information for CO_2 mole fraction and $\delta^{13}CO_2$ measurements made from NOAA flask air samples.
Table S2. Prior NEE, error covariance parameters, and background CO_2 mole fractions used in the 18 inversion ensemble members in this study.
Table S3. Correlations between prior and posterior NEE anomalies over North America and anomalies of area-weighted average precipitation, RH, VPD, and SM over temperate North America.
Table S4. Correlations between the ONI and 3-month average anomalies of area-weighted average air temperature, precipitation, RH, VPD, and SM over boreal and temperate North America.

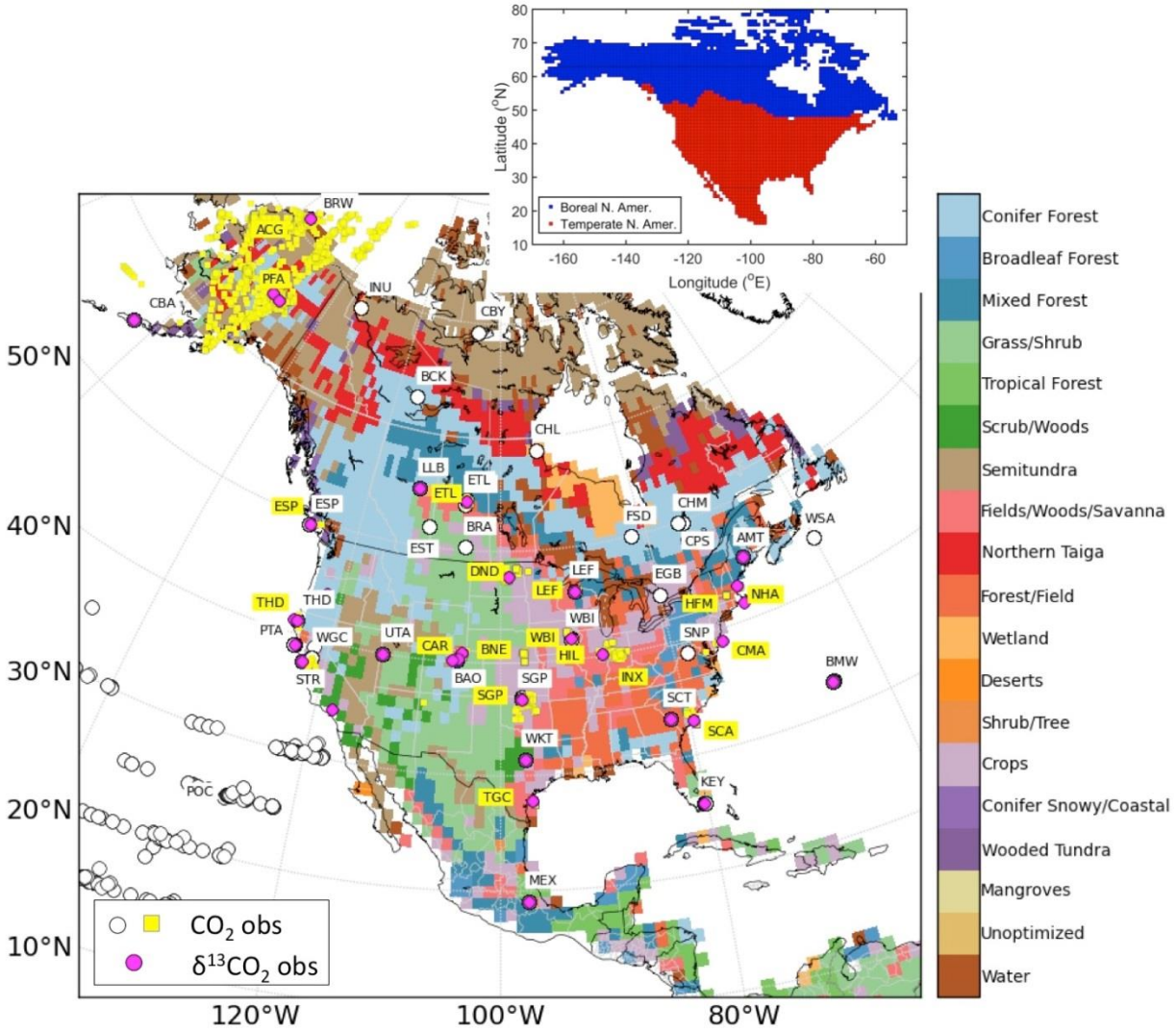

Fig. S1. Air sampling sites for measurements of atmospheric CO_2 mole fractions and $\delta^{13}CO_2$ under NOAA's Global Greenhouse Gas Reference Network between 2007 and 2015. Ground-based and airborne air-sampling sites for measurements of CO_2 are denoted by white circles and yellow squares, respectively. Measurements of $\delta^{13}CO_2$ were made only from NOAA's flask-air samples. Color shading indicates different eco-regions defined by Olson et al. (*55*). The subpanel on the upper right indicates boreal and temperate North America defined in the Atmospheric Tracer Transport Model Intercomparison (TransCom) Project (*56*) and used in this analysis.

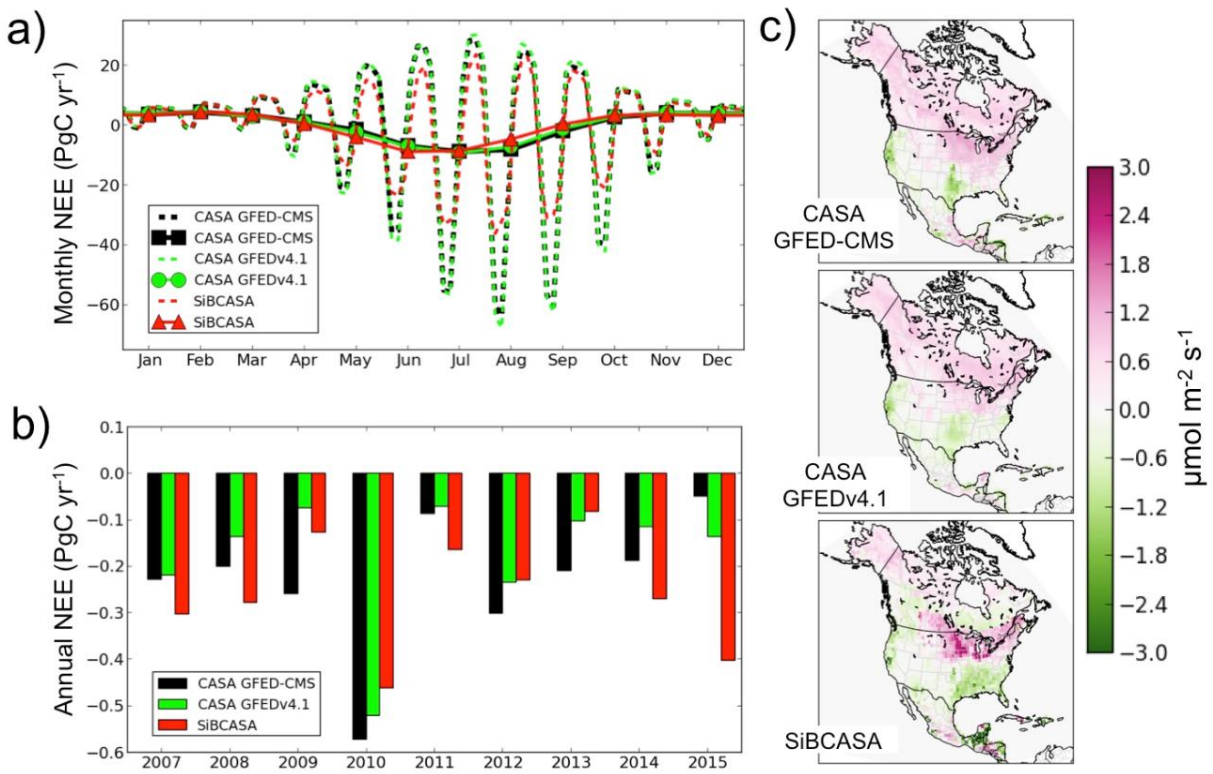

Fig. S2. Monthly and annual NEE used as prior fluxes in this study. Two of the prior fluxes are from CarbonTracker (CT2016)'s prior fluxes, which downscaled the monthly NEE from terrestrial biogeochemical models (CASA GFED-CMS and CASA GFEDv4.1s) to 3-hour resolution. The third prior fluxes are from a different process-based model SiBCASA, which explicitly calculates fluxes at hourly resolution. (a) Multi-year area-weighted average monthly NEE (solid symbols connected with solid lines) and multi-year area-weighted average monthly diurnal cycles of NEE (dashed lines) estimated from CT2016 and SiBCASA for North America. (b) Annual NEE from 2007 to 2015 from CASA GFED-CMS, CASA-GFEDv4.1s, and SiBCASA. (c) Multi-year averaged fluxes for April from three different prior NEE fluxes.

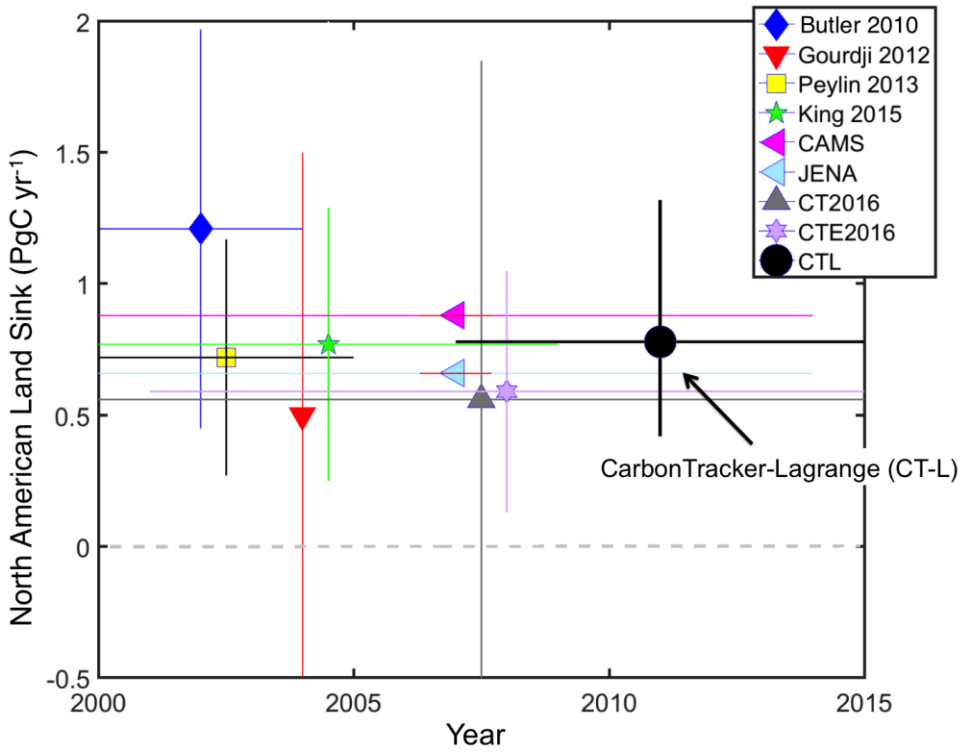

Fig. S3. Estimates of the North American land sink for 2000 to 2015 from published studies [Butler *et al*. (*19*), Gourdji *et al*. (*20*), and Peylin *et al*. (*18*), and King *et al*. (*17*)], recent releases of global inverse models (CAMS, Jena CarboScope, CT2016, and CTE2016), and from this study (CT-L). Vertical bars represent the estimated uncertainties from each study. Horizontal bars show the time period covered by each estimate.

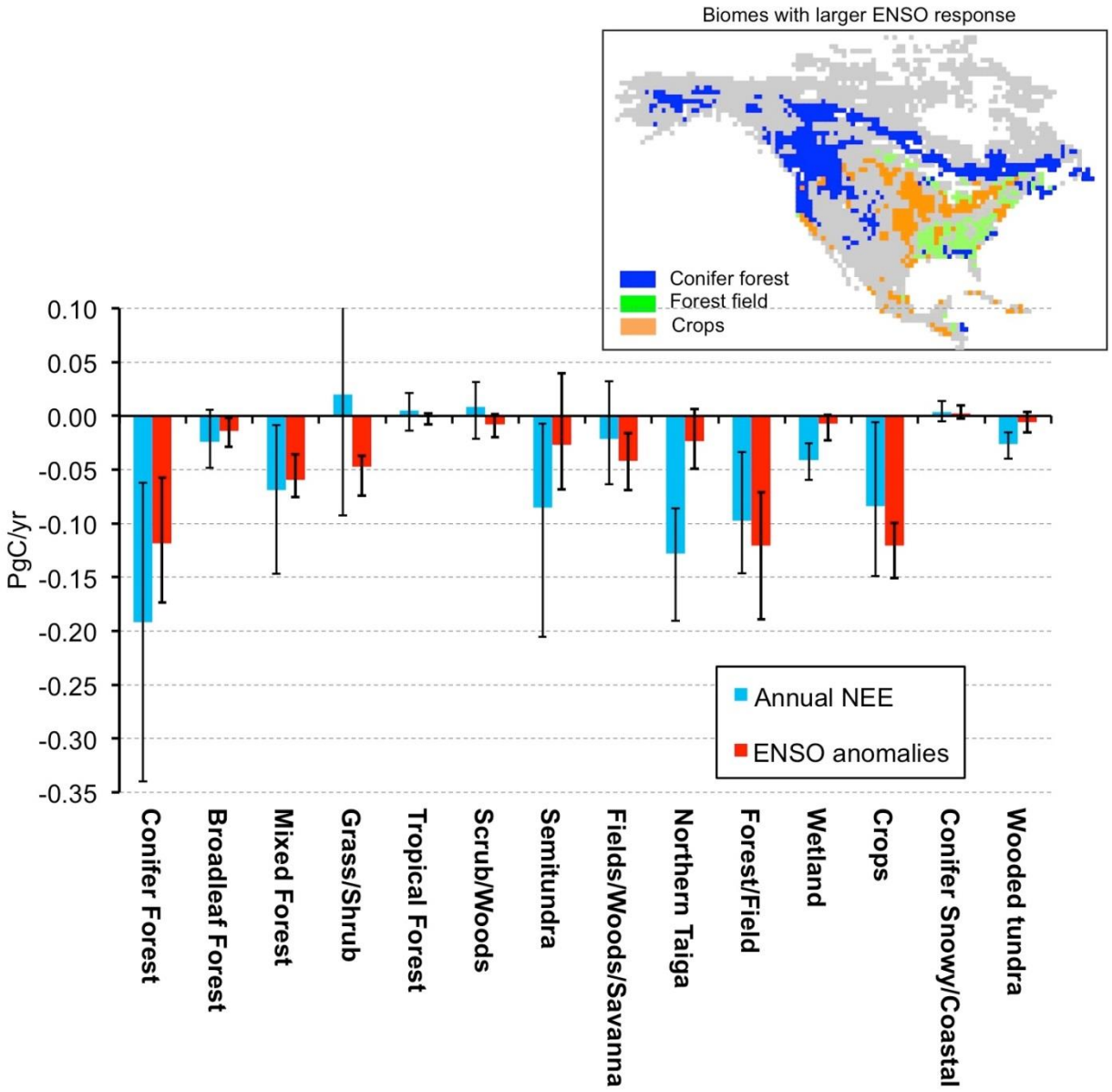

Fig. S4. Multiyear average annual NEE (blue bars) and differences of NEE anomalies between El Niño and La Niña periods (red bars) between 2007 and 2015 for different ecoregions defined in fig. S1. Errorbars for multi-year average NEE represent the range of 18 inversion estimates plus 2σ errors from each inversion. Errorbars for the ENSO anomalies represent the range estimated by 18 inversions. Ecoregions with larger ENSO response were indicated in the map on the upper right.

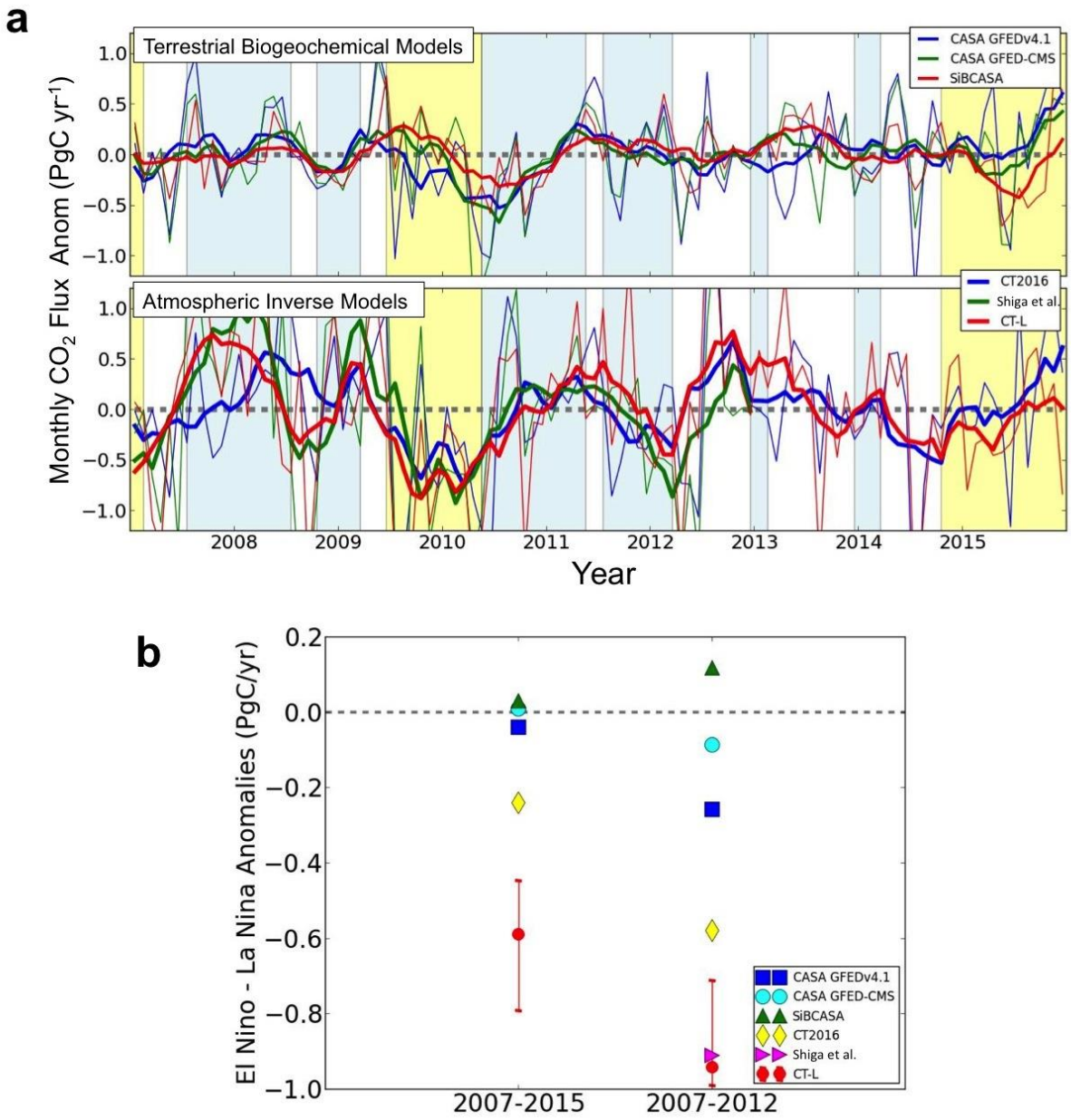

Fig. S5. IAV and ENSO response of North American NEE simulated by TBMs and atmosphere inverse models. (a) Interannual variability (monthly CO_2 flux anomalies) simulated by TBMs (CASA GFEDv4.1s, CASA GFED-CMS, SiBCASA) that were used as the prior fluxes of our estimate (a, upper panel) and inverse models (CarbonTracker (CT2016), high-resolution regional geostatistical inverse model (Shiga et al. (*21*)), and this study (CT-L). Thin lines indicate monthly anomalies, whereas thick lines represent 6-month running averages. Yellow and blue shadings indicate El Niño and La Niña periods. (b) The difference in average monthly anomalies between El Niño and La Niña periods for 2007 – 2015 and 2007 – 2012, estimated by TBMs and atmosphere inverse models.

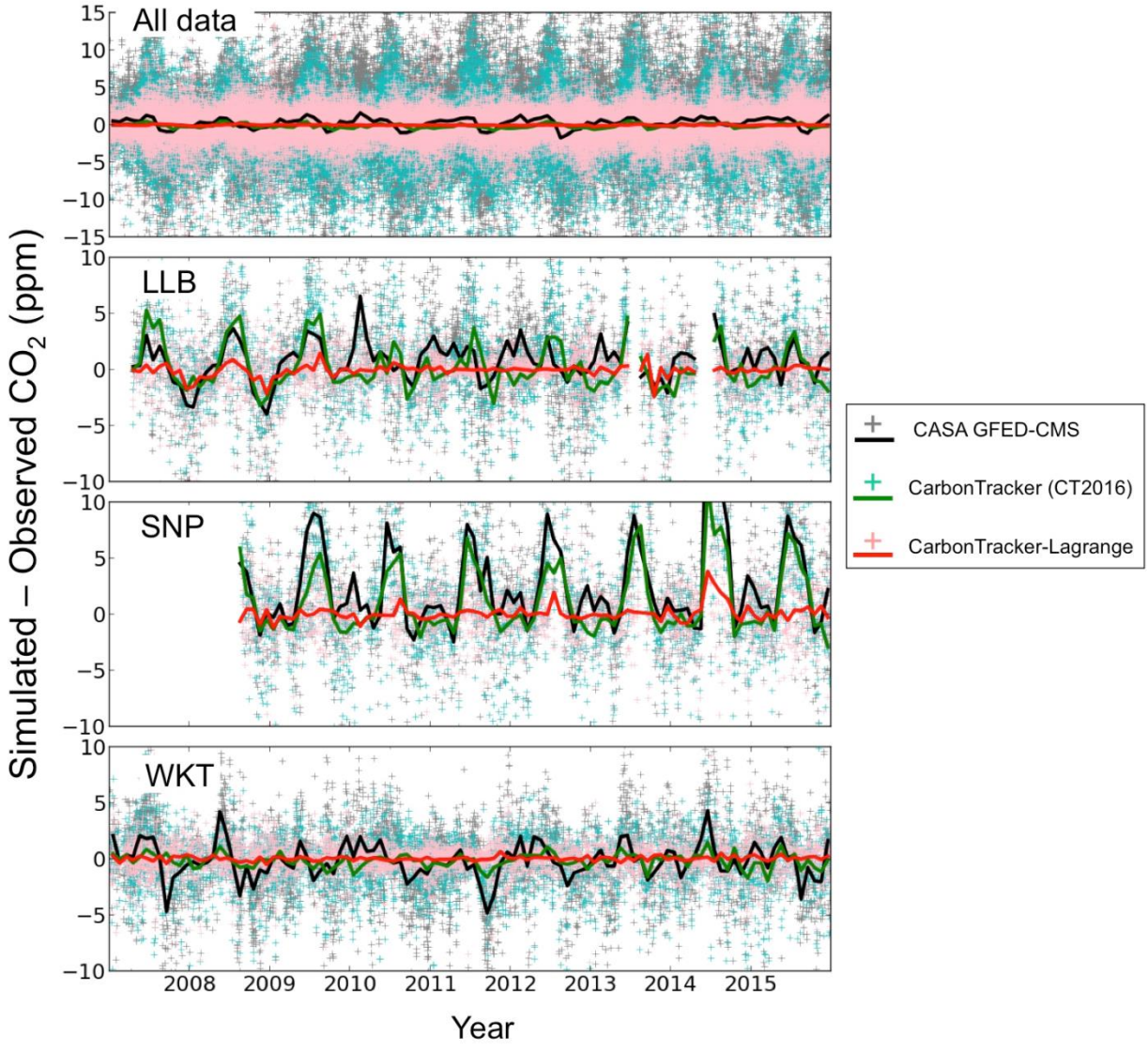

Fig. S6. Residuals between simulated and observed CO_2 mole fractions. (Top panel) Differences for all the observations included in inversions. (Middle to bottom panels) Differences for observations at selected sites. Symbols are residuals for individual observations whereas solid lines represent monthly average residuals. Gray symbols and black solid lines represent residuals using simulations with prior fluxes (CASA GFED-CMS) that were used in both CarbonTracker (CT2016) and CarbonTracker-Lagrange (CT-L). Green symbols and lines indicate residuals from the CT2016 simulation. Pink symbols and red lines indicate residuals from the CT-L simulation.

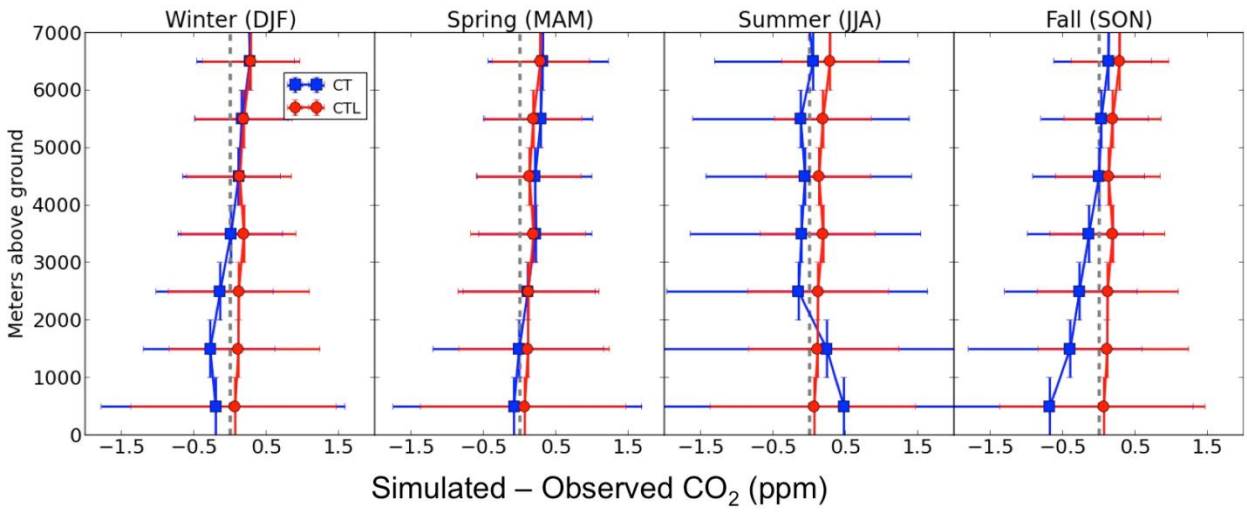

Fig. S7. Vertical profiles indicating seasonally averaged residuals (differences) between simulated and observed CO_2 mole fractions. Blue and red symbols indicate residuals from CT2016 (CT) and CarbonTracker-Lagrange (CT-L) simulations, respectively. The CT-L simulation shown above used the same prior fluxes as CT2016 and background values from CT2016. Horizontal bars indicate 1σ variability of the residuals. Vertical bars indicate vertical average intervals (which is every 1000 meters).

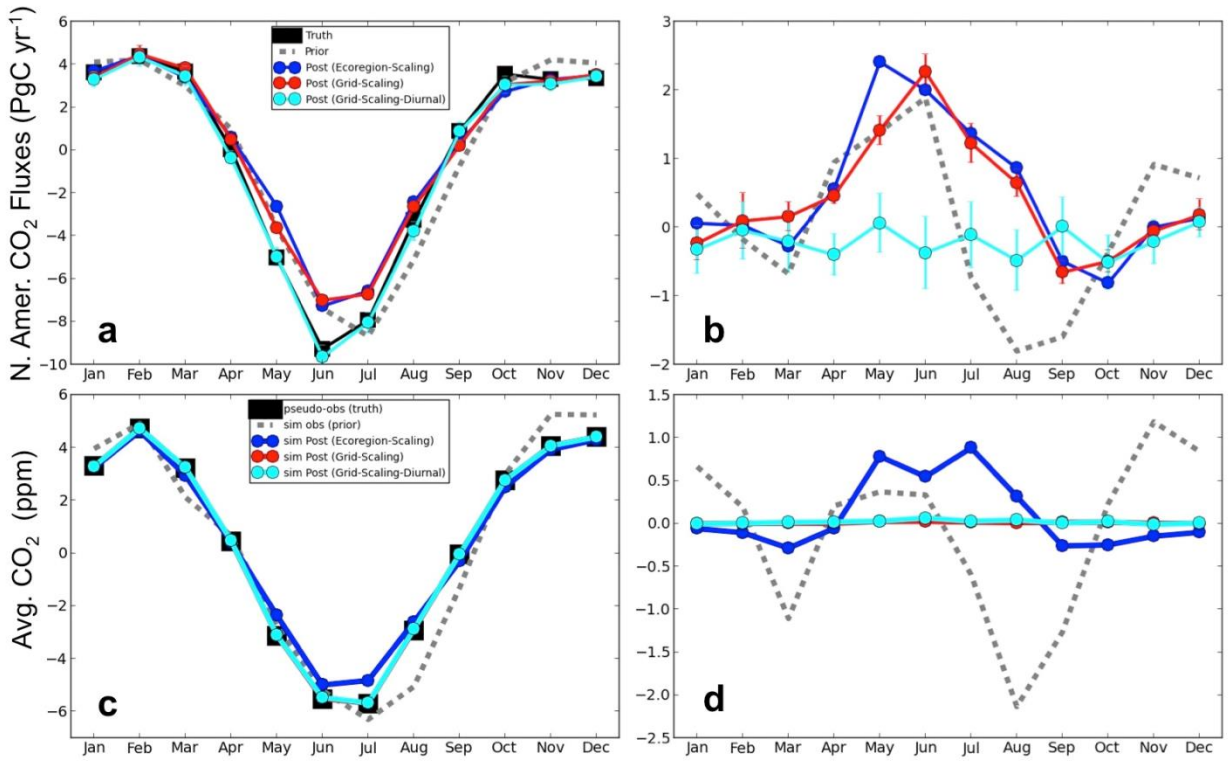

Fig. S8. Comparison of inversion results from OSSEs based on different model designs. (a) Comparison of derived North American CO_2 fluxes from OSSEs using pseudo observations created by convolving footprints with specified "true" fluxes. Specified true fluxes (black solid squares), prior fluxes (gray dashed lines), posterior fluxes derived from an ecoregion-based scaling on weekly fluxes (blue symbols connected with blue solid lines), a grid-scale-based scaling on weekly fluxes (red symbols connected with red solid lines), and a grid-scale-based scaling on weekly fluxes including adjustment of the diurnal cycle of CO_2 fluxes (cyan symbols connected with cyan solid lines). (b) Differences of prior and posterior fluxes with synthetic true fluxes in the OSSEs. (c) Monthly ΔCO_2 mole fraction averaged across all North American sites, computed using true, prior and posterior fluxes shown in the upper panel, where ΔCO_2 denotes the mole fraction deviations due to surface fluxes over the ten days prior to the simulated measurement. (d) Differences between simulated and pseudo observations using prior and posterior fluxes.

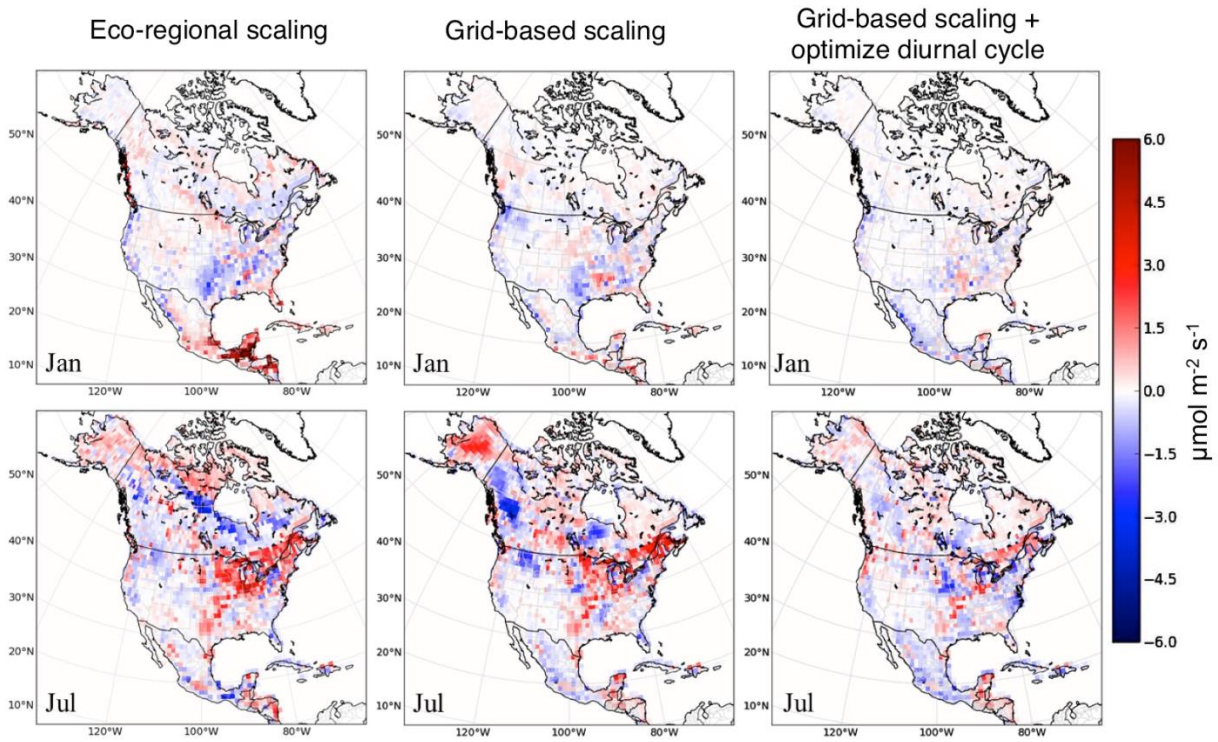

Fig. S9. Differences between posterior and true fluxes derived from observing system simulation experiments. (Upper panels) Differences for fluxes in January. (Lower panels) Differences for fluxes in July. Panels from left to right used posterior fluxes derived from ecoregion-based scaling on weekly fluxes, grid-scale-based scaling on weekly fluxes, and grid-scale-based scaling on weekly fluxes including optimization of the diurnal cycle of CO_2 fluxes.

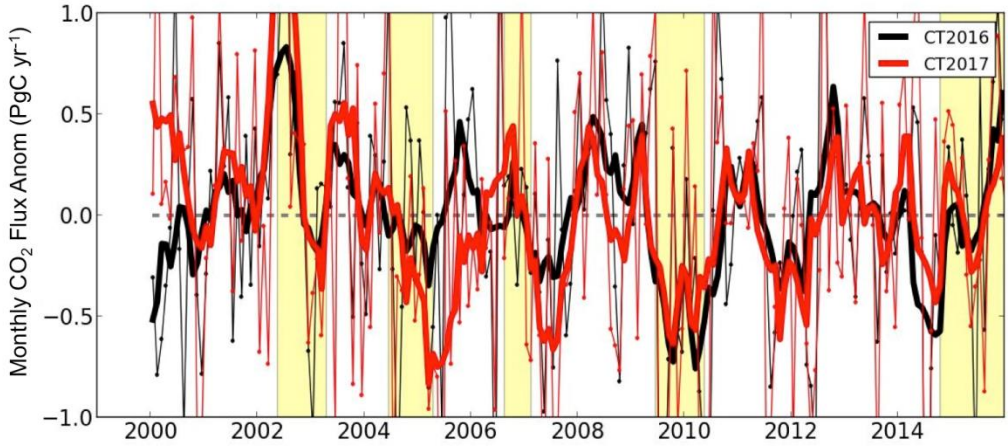

Fig. S10. Anomalies of NEE for North America derived from CarbonTracker (CT2016: black; CT2017: red). CT2016 and CT2017 fluxes were derived with similar inversion configurations. However, the number of atmospheric CO_2 observations used in CT2017 is one order of magnitude larger than that in CT2016. Thin lines represent monthly anomalies and thick lines represent their 6-month running averages. Yellow shading represents El Niño periods.

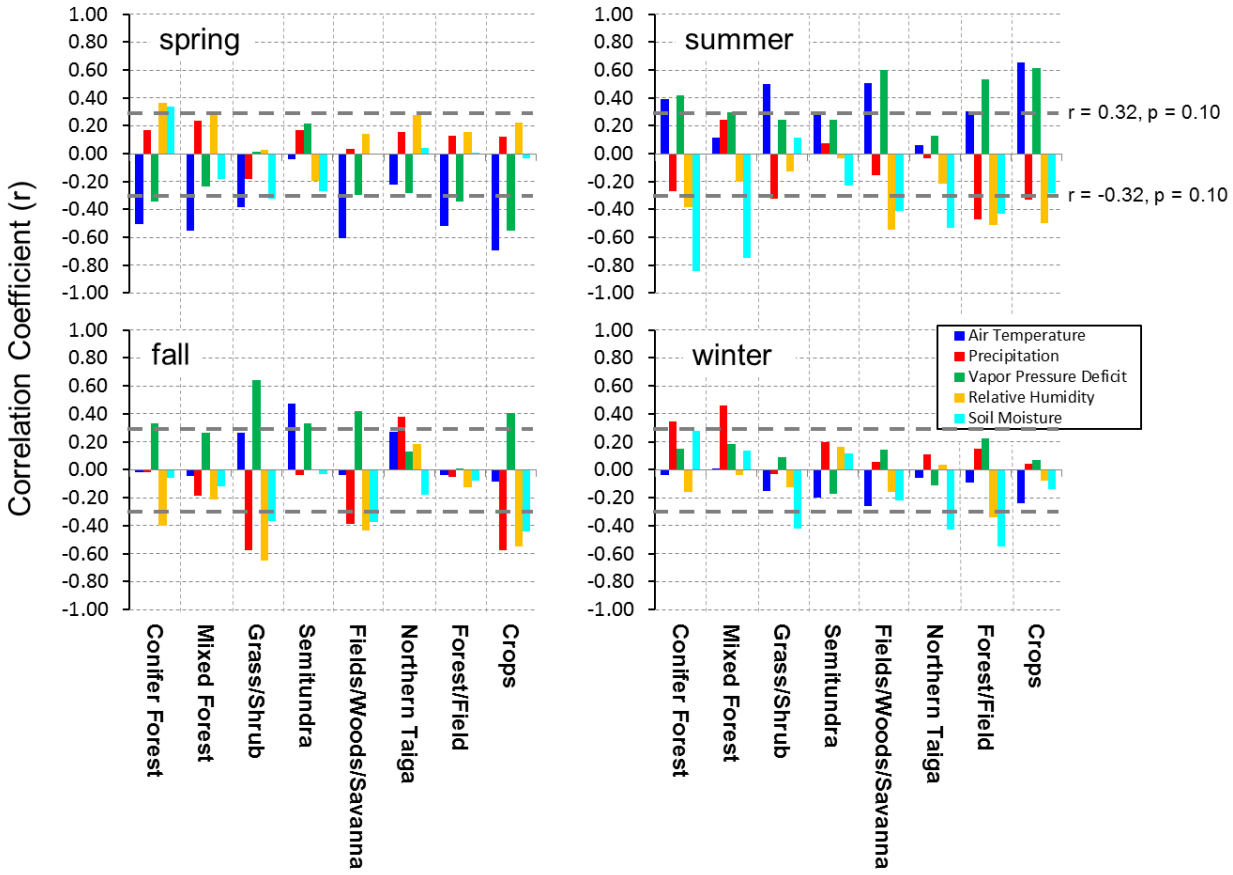

Fig. S11. Correlation coefficients between NEE anomalies and anomalies of air temperature, precipitation, VPD, RH, and SM for spring (March to May), summer (June to August), fall (September to November), and winter (December to February) for major biome types over North America that have larger carbon uptake (indicated in fig. S4). Correlations above or below the gray dash lines are significant at a 90% confidence interval.

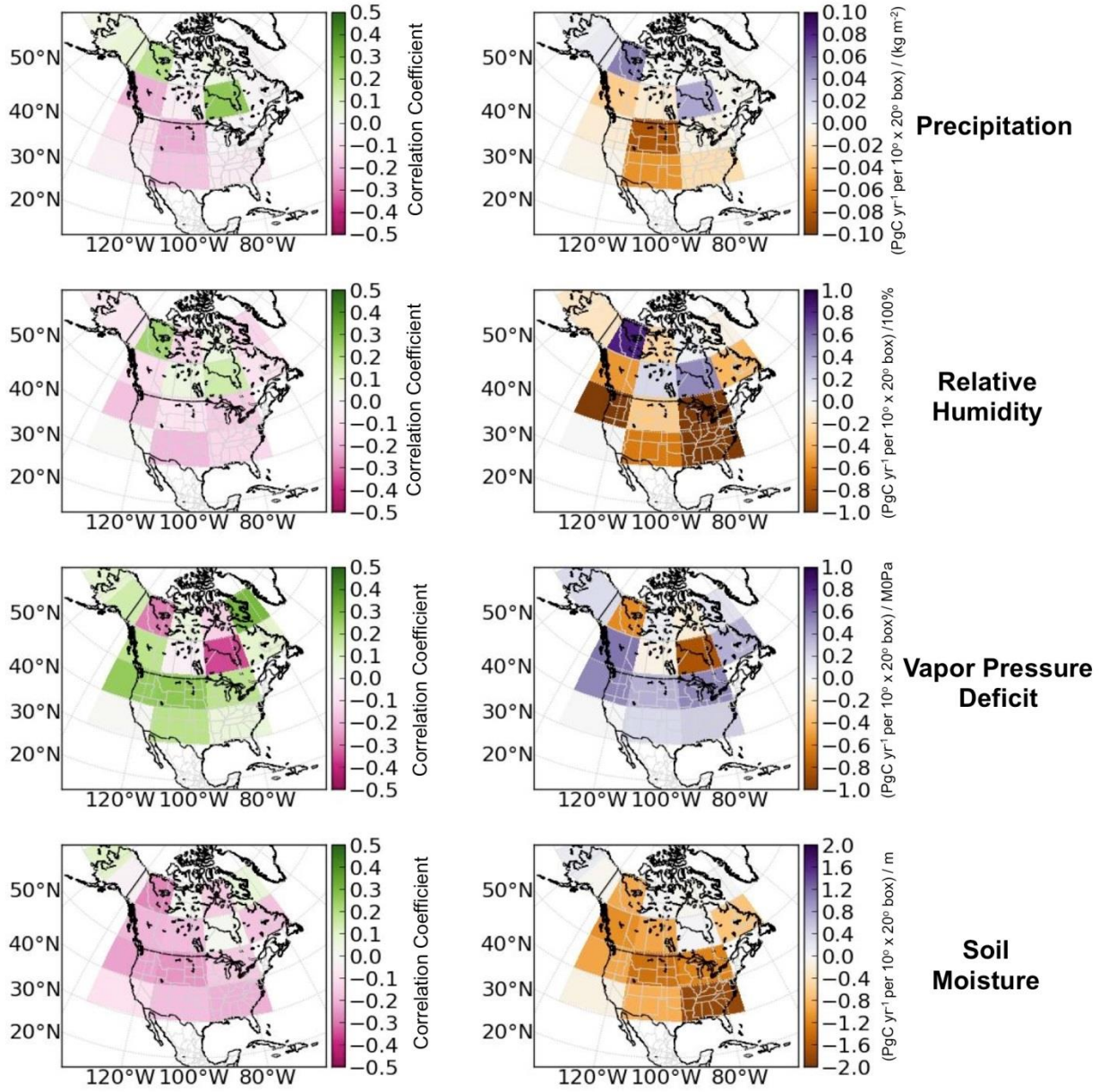

Fig. S12. Correlations between monthly NEE anomalies and monthly anomalies of hydrological variables (precipitation, relative humidity, vapor pressure deficit, and soil moisture) and the sensitivity of NEE anomalies to hydrological conditions. (Left panels) Correlation coefficients between monthly NEE anomalies and monthly anomalies of hydrological variables (precipitation, relative humidity, vapor pressure deficit, and soil moisture) with NEE lagging climate variables by 1 month between 2007 and 2015. (Right panels) The sensitivity of NEE anomalies to variability of hydrological variables (calculated as slopes of their linear regressions). The number of data points included in these calculations is 107. Correlation coefficients that have an absolute value larger than 0.16 indicate significant correlations at a 90% confidence interval.

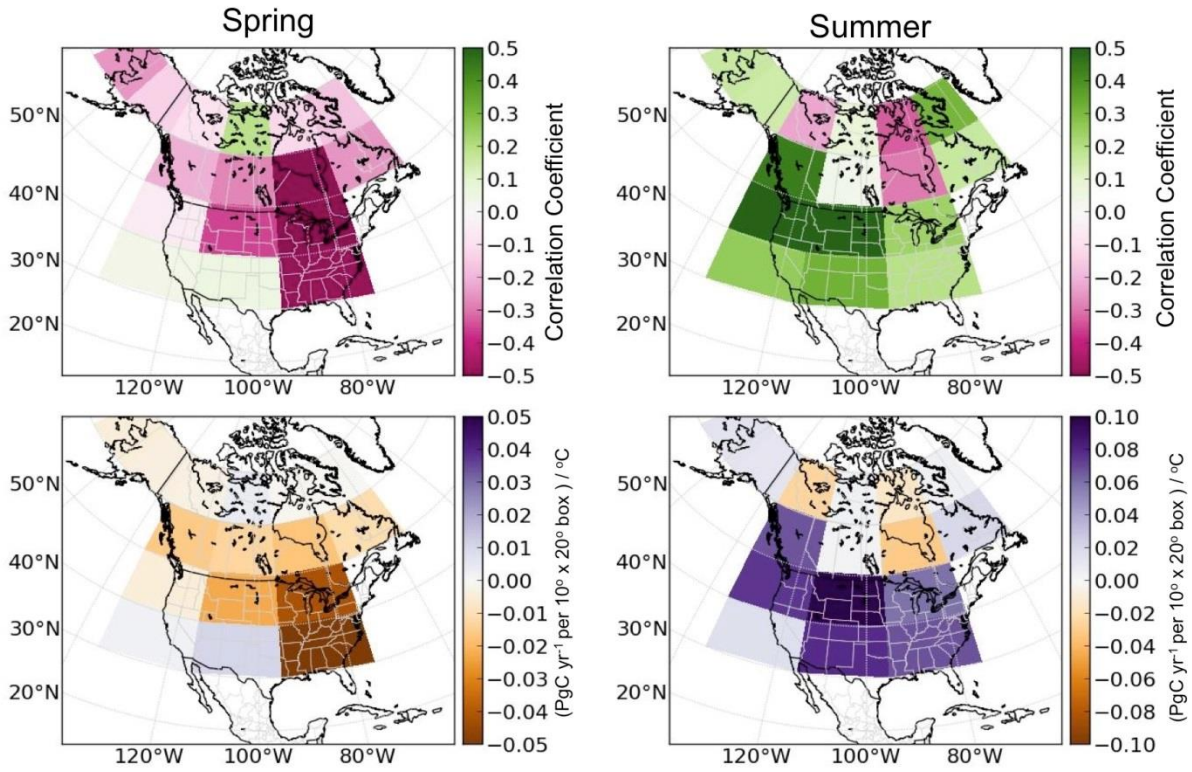

Fig. S13. Correlations between NEE anomalies and anomalies of air temperature in spring and summer, and the sensitivity of NEE anomalies to air temperature. (Top panels) Correlation coefficients between NEE anomalies and anomalies of air temperature for spring and summer. (Lower panels) Sensitivities of NEE anomalies to anomalies of air temperature, as indicated by the slopes of their linear regression. The number of data points included in the correlation is 27. Correlation coefficients that have an absolute value larger than 0.32 indicate significant correlations at a 90% confidence interval.

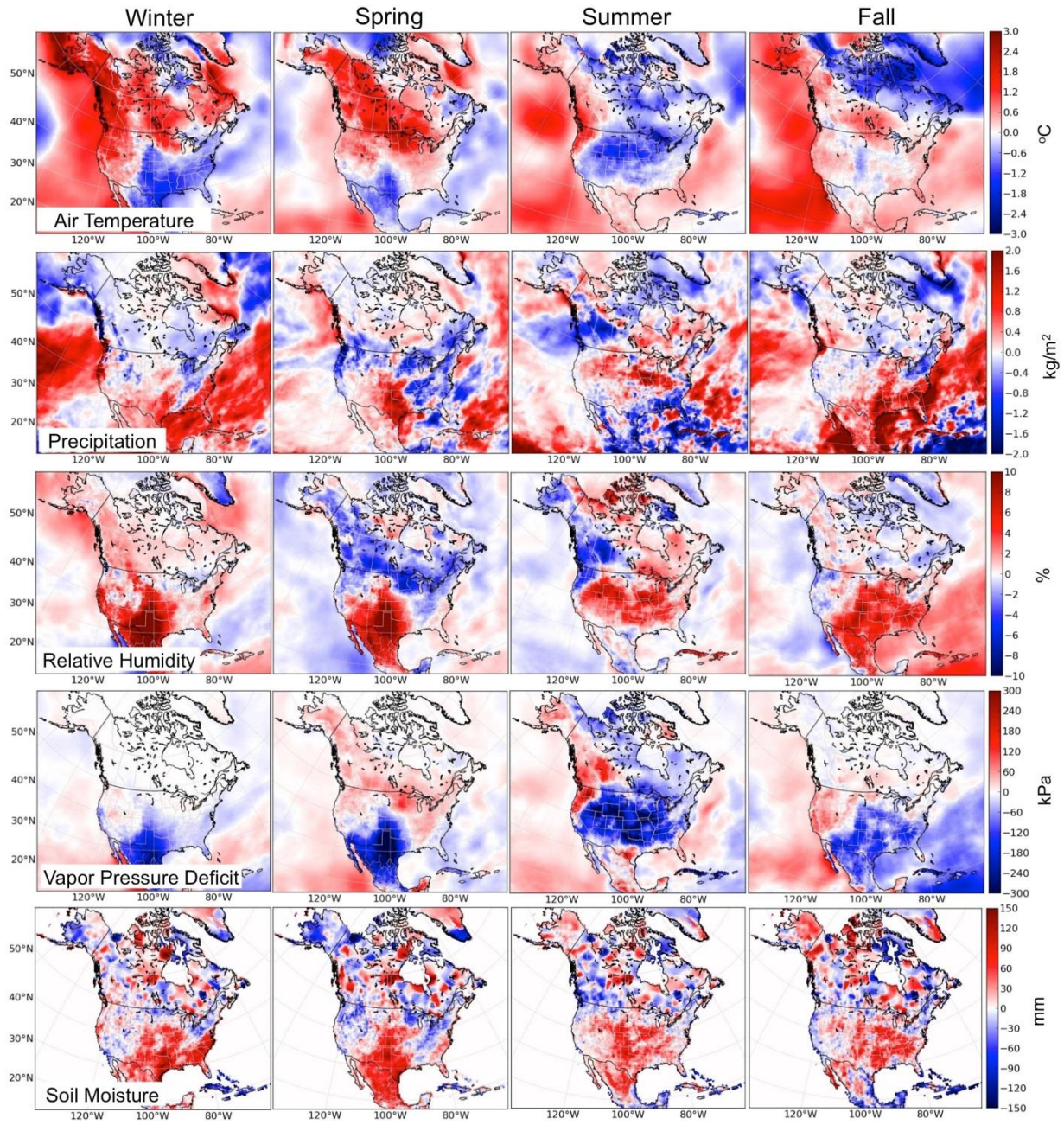

Fig. S14. Difference of anomalies of air temperature, precipitation, relative humidity, vapor pressure deficit, and soil moisture between El Niño and non El Niño (neutral and La Niña) periods.

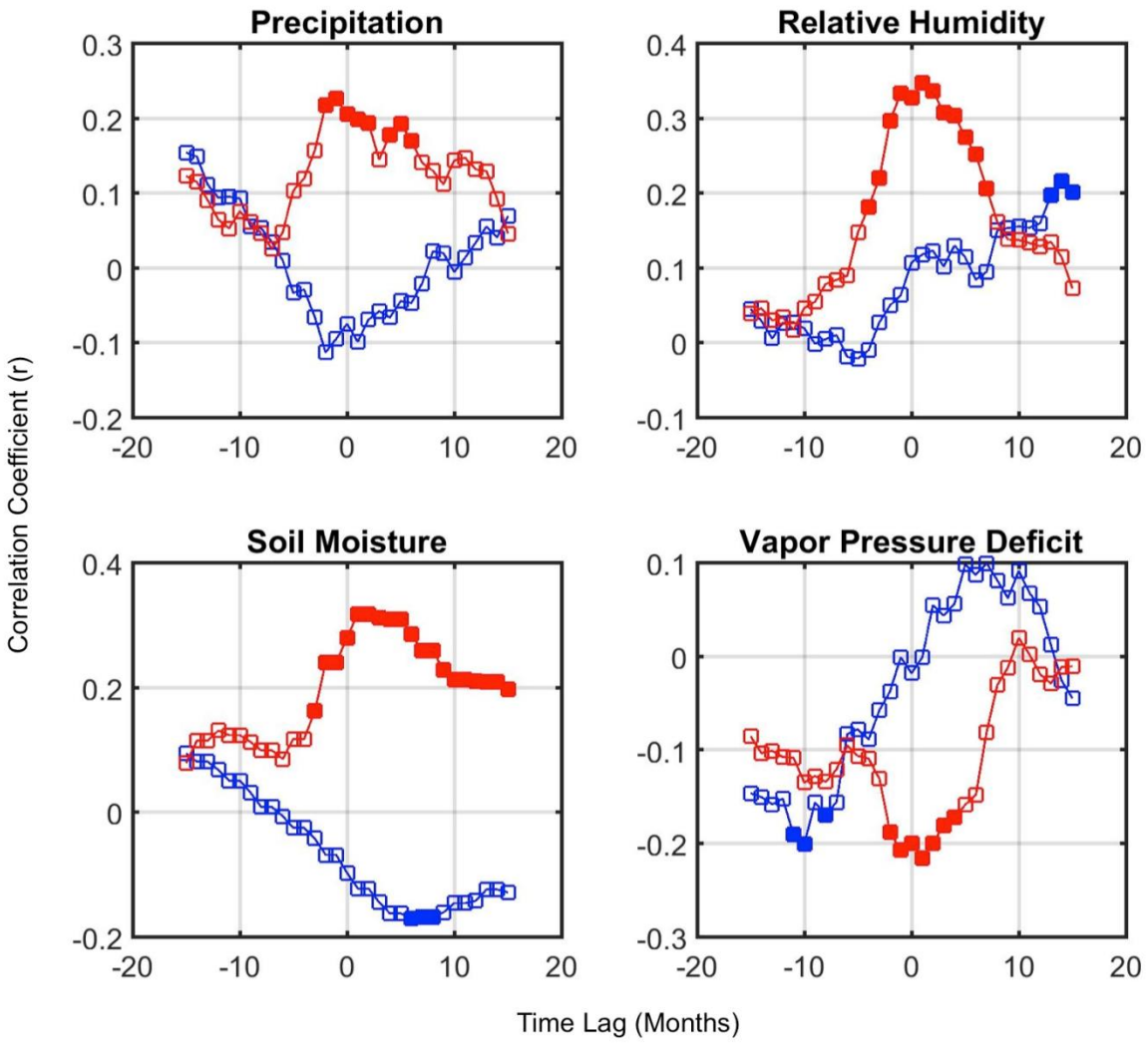

Fig. S15. Correlations between the ONI and 3-month average anomalies of area-weighted average precipitation, RH, SM, and VPD over boreal (blue symbols) and temperate (red symbols) North America with ±10-month time lags. Filled symbols indicate statistically significant correlations at a 95% confidence interval ($p<0.05$) whereas empty symbols indicate insignificant correlations.

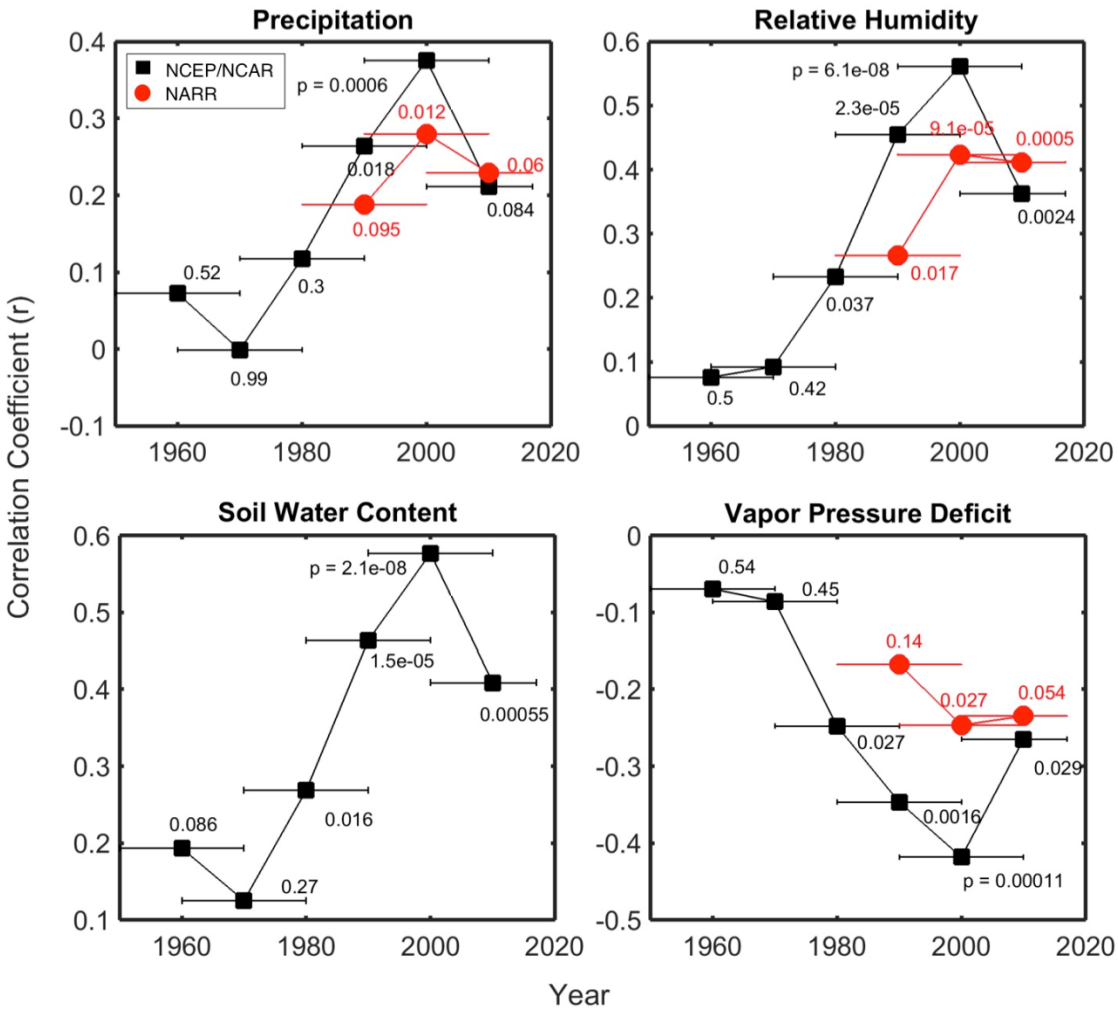

Fig. S16. Correlations between the ONI and 3-month average anomalies of area-weighted average precipitation, RH, SM, and VPD over temperate North America for every 20 years between 1950 and 2016. Black symbols indicate correlations calculated using the NCEP/NCAR reanalysis data and red symbols indicate correlations calculated using the North American Regional Reanalysis (NARR) data. Each point is labeled with its p-value of the correlation. Horizontal bars denote the time periods that the correlations represent.

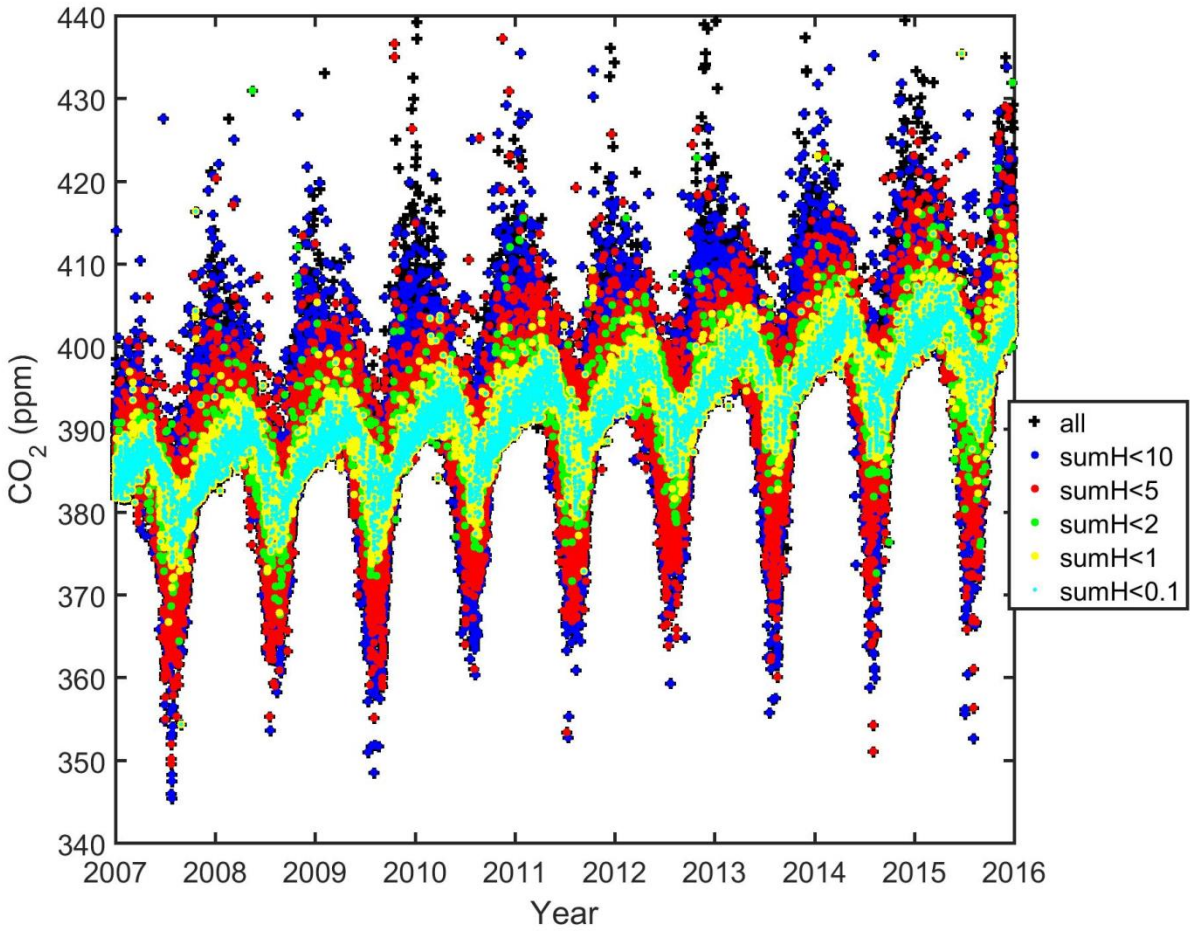

Fig. S17. Atmospheric CO_2 observations between 2007 and 2015 with different colors indicating their total sensitivity [sumH, ppm (μmol m^{-2} s^{-1})$^{-1}$] to North American land fluxes. When the total sensitivity (sumH) was low, observations were less influenced by North American land fluxes than for larger sumH.

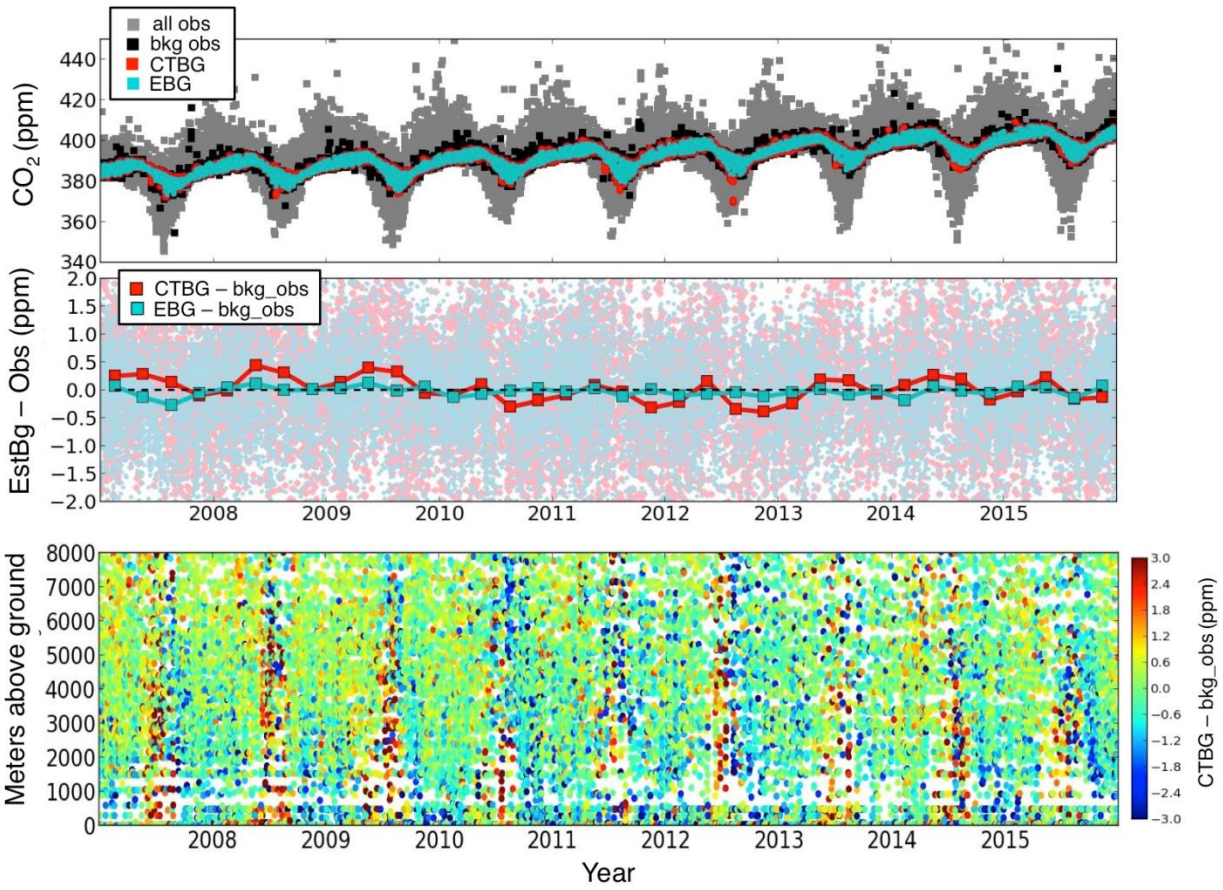

Fig. S18. Observed CO_2 mole fractions for observations used in this analysis and their associated background estimates. (Upper) CO_2 observations between 2007 and 2015 (gray), observations with low influence by land fluxes (summed footprint ≤ 1 ppm (μmol m^{-2} s^{-1})$^{-1}$) or background observations (black), estimated background mole fractions using CT2016's 4D CO_2 simulations (CTBG, red) and an empirical method (EBG, cyan). (Middle) Differences between estimated (CTBG and EBG) and observed background for background observations. Lighter colored symbols are raw differences. Darker colored symbols connected with solid lines indicate 3-monthly average differences. (Lower) Differences between estimated background (CTBG) and observations for the selected background observations (summed footprint ≤ 1 ppm (μmol m^{-2} s^{-1})$^{-1}$) along altitudes.

Table S1. Site information for CO_2 mole fraction and $\delta^{13}CO_2$ measurements made from NOAA flask air samples.

Site	Latitude	Longitude	Period of operation	Site	Latitude	Longitude	Period of operation
AAO	40.14	-88.57	2006 - 2010	LLB	54.95	-112.45	2008 - 2013
AMT	45.03	-68.68	2004 - 2018	MBO	43.98	-121.69	2012 - present
BAO	40.05	-105	2008 - 2017	MEX	18.98	-97.31	2008 - present
BNE	40.74	-97.18	2005 - 2011	MWO	34.22	-118.06	2010 - present
BRW	71.32	-156.6	1971 - present	NHA	42.94	-70.6	2004 - present
CAR	40.82	-104.65	1993 - present	NWR	40.05	-105.6	1968 - present
CBA	55.2	-162.72	1979 - present	PFA	64.81	-148.04	2000 - present
CMA	38.86	-74.34	2006 - present	PTA	38.95	-123.73	1999 - 2011
CRV	64.58	-149.18	2011 - present	SCA	32.84	-79.49	2004 - present
DND	47.7	-98.73	2005 - present	SCT	33.41	-81.83	2009 - present
ESP	49.38	-126.54	2003 - present	SGP	36.63	-97.51	2003 - present
ETL	54.32	-104.97	2006 - present	STR	37.76	-122.45	2008 - present
HFM	42.54	-72.17	2000 - present	TGC	27.69	-96.75	2004 - present
HIL	40.05	-87.93	2005 - present	THD	41.04	-124.15	2002 - present
INX	39.03	-91.08	2011 - 2016	UTA	39.9	-113.72	1993 - present
ITN	35.37	-77.39	1993 - 1999	WBI	41.75	-91.37	2005 - present
KEY	25.67	-80.19	1973 - present	WGC	38.26	-121.38	2008 - present
LEF	45.94	-90.26	1995 - present	WKT	31.32	-97.33	2001 - present
LEW	40.94	-76.88	2013 - present				

Table S2. Prior NEE, error covariance parameters, and background CO_2 mole fractions used in the 18 inversion ensemble members in this study. The 3-hourly prior NEE were from CarbonTracker (CT2016) prior NEE and from the Combined Simple Biosphere/Carnegie-Ames-Stanford Approach terrestrial carbon cycle model (SiBCASA). CT2016 prior fluxes were obtained by downscaling monthly NEE from process-based terrestrial biogeochemical models (CASA GFED-CMS and CASA GFEDv4.1s) to 3-hourly NEE fluxes, whereas SiBCASA simulates diurnal cycle of ecoregion respiration and gross primary production explicitly. Error covariance parameters were derived from maximum likelihood estimation (MLE) with fixed correlation scales (1000 km and 7 days) or optimized correlation scales. Background CO_2 mole fractions were derived from three different approaches: (1) extracted from the 4D CarbonTracker-simulated CO_2 mole fraction field (CTBG), (2) extracted from a 4D CO_2 mole fraction field constructed from an empirical method (EBG), and (3) background estimated from CTBG and corrected using a subset of background CO_2 observations that have minimum sensitivity to the North American land ($CTBG_{corr}$).

Prior Fluxes	**Error Covariance Parameters** [a]	**Background CO_2 Mole Fractions**		
		CTBG	**EBG**	**$CTBG_{corr}$**
CT2016 Prior 1 (CASA GFED-CMS)	MLE-Determined Seasonal σ_r and σ_q (τ_s = 1000 km, τ_t = 7 days)	×	×	×
	MLE-Determined Seasonal σ_r, σ_q, τ_s, τ_t (τ_s = 263 - 439 km, τ_t = 28 - 51 days)	×	×	×
CT2016 Prior 2 (CASA GFEDv4.1)	MLE-Determined Seasonal σ_r and σ_q (τ_s = 1000 km, τ_t = 7 days)	×	×	×
	MLE-Determined Seasonal σ_r, σ_q, τ_s, τ_t (τ_s = 308 - 527 km, τ_t = 18 - 55 days)	×	×	×
SiBCASA	MLE-Determined Seasonal σ_r and σ_q (τ_s = 1000 km, τ_t = 7 days)	×	×	×
	MLE-Determined Seasonal σ_r, σ_q, τ_s, τ_t (τ_s = 207 - 357 km, τ_t = 22 - 44 days)	×	×	×

Note:

[a] σ_r represents model-data mismatch errors (in ppm) at individual CO_2 measurement sites; σ_q represents relative prior flux errors associated with each prior flux field; τ_s and τ_t are the e-folding correlation scales in space and time associated with estimated relative prior flux errors.

Table S3. Correlations between prior and posterior NEE anomalies over North America and anomalies of area-weighted average precipitation, RH, VPD, and SM over temperate North America. The correlations below are correlation coefficients with p-value included in parentheses. These correlations were calculated with fluxes lagging climate variables by 0 – 3 months. The number of data points included in the calculation is indicated as the n value.

Climate Variables	Prior (Time Lag = 1 month, n = 107)			Posterior			
	CASA GFED-CMS	CASA GFEDv4.1s	SiBCASA	Time Lag = 0 month (n=108)	Time Lag = 1 month (n=107)	Time Lag = 2 months (n=106)	Time Lag = 3 months (n=105)
Air Temperature	-0.003(0.98)	-0.09 (0.34)	-0.005 (0.96)	-0.03 (0.76)	-0.01 (0.90)	0.13 (0.17)	0.13 (0.19)
Precipitation	-0.05 (0.62)	-0.03 (0.78)	0.12 (0.22)	0.09 (0.34)	-0.21 (0.03)	-0.17 (0.09)	-0.17 (0.09)
Relative Humidity	-0.14 (0.15)	-0.14 (0.15)	-0.04 (0.69)	-0.17 (0.085)	-0.38 (<0.0001)	-0.32 (0.0008)	-0.15 (0.13)
Vapor Pressure Deficit	0.16 (0.10)	0.16 (0.09)	0.09 (0.34)	0.24 (0.01)	0.39 (<0.0001)	0.31 (0.001)	0.17 (0.08)
Soil Moisture	-0.15 (0.14)	-0.23 (0.02)	-0.25 (0.01)	-0.29 (0.004)	-0.32 (0.001)	-0.25 (0.01)	-0.17 (0.09)

Table S4. Correlations between the ONI and 3-month average anomalies of area-weighted average air temperature, precipitation, RH, VPD, and SM over boreal and temperate North America. Correlations shown below are correlation coefficients with p-values included in parentheses.

	Boreal North America	**Temperate North America**
Air temperature	0.11 (0.17)	0.07 (0.37)
Precipitation	-0.07 (0.37)	0.21 (0.01)
Relative humidity	0.11 (0.19)	0.31 (0.0001)
Vapor pressure deficit	-0.02 (0.84)	-0.19 (0.02)
Soil Moisture	-0.10 (0.24)	0.28 (0.0006)